Dynamics of a Cold Trapped Ion in a Bose-Einstein Condensate

Stefan Schmid,[1,2] Arne Härter,[1,2] and Johannes Hecker Denschlag[1,2]

[1]*Institut für Quantenmaterie, Universität Ulm, 89069 Ulm, Germany*

[2]*Institut für Experimentalphysik und Zentrum für Quantenphysik, Universität Innsbruck, 6020 Innsbruck, Austria*

(Received 27 July 2010; published 23 September 2010)

We investigate the interaction of a laser-cooled trapped ion (Ba^+ or Rb^+) with an optically confined ^{87}Rb Bose-Einstein condensate. The system features interesting dynamics of the ion and the atom cloud as determined by their collisions and their motion in their respective traps. Elastic as well as inelastic processes are observed and their respective cross sections are determined. We demonstrate that a single ion can be used to probe the density profile of an ultracold atom cloud.

DOI: 10.1103/PhysRevLett.105.133202 PACS numbers: 34.50.−s, 03.75.Hh, 34.70.+e, 37.10.−x

The realization of a charged quantum gas, formed by laser-cooled, trapped ions and ultracold neutral atoms, offers intriguing perspectives for a variety of novel experiments. In addition to studying atom-ion collisions and chemical reactions in a regime where only one or few partial waves contribute, interesting phenomena such as charge transport in the ultracold domain [1], polaron-type physics [2–4], and novel atom-ion bound states [5] can be investigated. Furthermore, the production of cold, charged molecules in a well-defined quantum state is an important goal in molecular physics [6,7]. Techniques and tools that are widely used to control neutral atomic quantum gases, e.g., Feshbach resonances [8], may be employed in atom-ion collisions as well [9]. First observations of cold collisions with trapped atoms and ions in the mK regime have been made by using Yb^+ ions and a magneto-optical trap for Yb [10,11] and very recently with a Bose-Einstein condensate (Yb^+ and Rb) [12,13]. Here we present our investigations where we use a defined small number of Ba^+ or Rb^+ ions which are immersed in an ultracold cloud of Rb atoms, which is either Bose-Einstein condensed or at sub-μK temperature. The elastic cross sections are large as expected. Inelastic processes are, in general, strongly suppressed, which is important for planned future experiments. Charge transfer is directly identified in our experiments and found to be the dominant inelastic collision channel. As a first application we show how a trapped ion can be used to locally probe the density profile of a condensate. In our experiment we find the micromotion of the trapped ion to play an important role for the atom-ion dynamics.

In the inhomogeneous electrical field of an ion, a neutral atom is polarized and attracted towards the ion. This interaction can be expressed as a long-range polarization potential $V(r) = -C_4/2r^4$ with $C_4 = q^2\alpha/4\pi\epsilon_0$, where q is the charge of the ion and α the dc polarizability of the atom. The characteristic radius of the potential is given by $r^* = \sqrt{\mu C_4/\hbar}$, where μ is the reduced mass. For a ^{87}Rb atom ($\alpha = 4.7 \times 10^{-31}$ m^3 [14]) interacting with a $^{138}Ba^+$ ion, this characteristic radius is $r^* = 295$ nm. This is much larger than the typical length scale of the neutral atom-atom interaction potential as given by the van der Waals radius, which for ^{87}Rb is $R_{\mathrm{vdW}} \approx 4$ nm [8]. For collision energies E above $k_B \times 100$ μK, the cross section for elastic scattering can be approximated by the semiclassical estimate $\sigma_{\mathrm{el}} = \pi(\mu C_4/\hbar^2)^{1/3}(1 + \pi^2/16)E^{-1/3}$ [15]. At lower energies a full quantum mechanical treatment is necessary, which takes into account individual partial waves. In addition to elastic collisions, inelastic processes can also occur, such as charge transfer $Rb + Ba^+ \rightarrow Rb^+ + Ba$ or molecule formation $Rb + Rb + Ba^+ \rightarrow Rb + (BaRb)^+$.

Here we present the first results obtained with our novel hybrid apparatus, where both species (Ba^+ and Rb) are first trapped and cooled in separate parts of a UHV chamber in order to minimize mutual disturbance and are then brought together. We use a linear Paul trap into which we can load a well-defined number of $^{138}Ba^+$ ions (typically 1) by photoionizing neutral Ba atoms from a getter source. Photoionization is done with a diode laser at 413 nm, which drives a resonant two-photon transition from the ground state to the continuum via the $^3D_1$ state. The $^{138}Ba^+$ ion which has no hyperfine structure is Doppler-cooled to mK temperatures by using a laser at 493 nm. Another laser at 650 nm repumps from a metastable $D_{3/2}$ state. The ion's fluorescence is collected with a lens of N.A. = 0.2 and then detected by using an electron multiplying charged-coupled device camera. The linear Paul trap (see Fig. 1) consists of four blade electrodes, which are placed at a distance of 2 mm from the trap axis, and two end cap electrodes at a distance of 7 mm from the trap center. It is operated with a radio frequency (rf) drive of $\Omega = 2\pi \times 5.24$ MHz with an amplitude of 1400 Vpp and a dc end cap voltage of about 100 V. With these parameters we measure the axial and the radial trap frequencies to be $\omega_{I,\mathrm{ax}} \approx 2\pi \times 80$ kHz and $\omega_{I,\mathrm{rad}} \approx 2\pi \times 200$ kHz, respectively.

The sample of ultracold Rb atoms is prepared similarly as described in Ref. [16]. Atoms from a magneto-optical trap are magnetically transferred over a distance of 43 cm into a quadrupole Ioffe configuration trap. Evaporative cooling yields a cloud of 3×10^6 ^{87}Rb atoms in state $|F = 1, m_F = -1\rangle$ at a temperature of about 1 μK. From

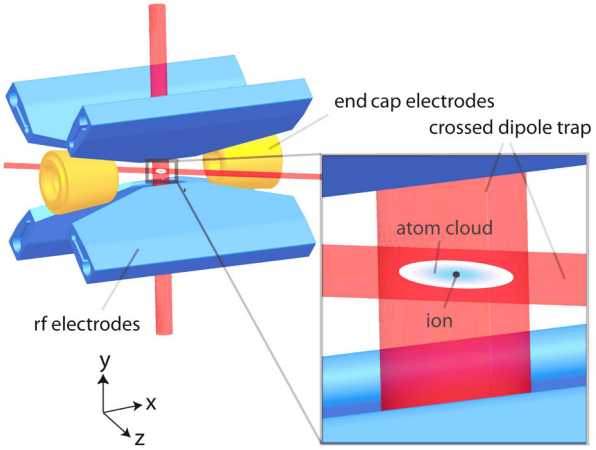

FIG. 1 (color online). Combined atom-ion trap: A linear radio frequency Paul trap is used to store ions [20], whereas the ultracold atoms are confined in a crossed optical dipole trap. By precisely overlapping the positions of these two traps, a single ion can be immersed into the center of the ultracold neutral atom cloud.

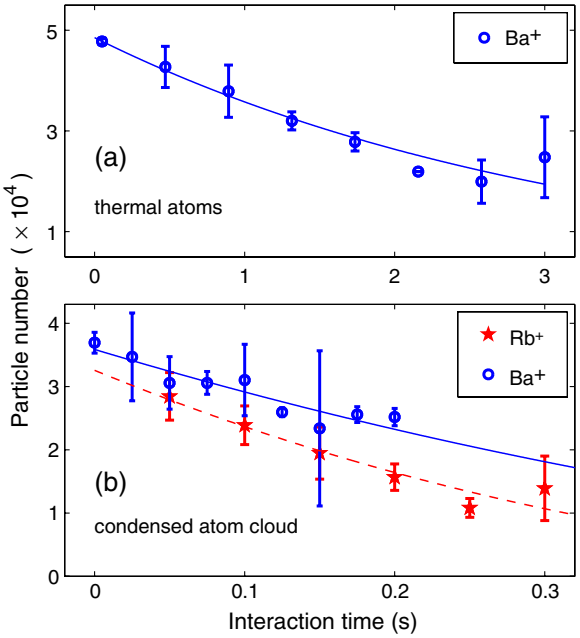

FIG. 2 (color online). Number of remaining Rb atoms as a function of time as a sample of Rb atoms interacts with an ion. (a) A single Ba^+ ion is immersed into the center of a thermal Rb cloud. The line is an exponential decay fit. (b) A single ion (Ba^+ or Rb^+) is immersed in a Rb Bose-Einstein condensate. The lines are fits based on our simple model described in the text.

the magnetic trap we load the atom cloud into a vertical 1-dimensional optical lattice trap formed by two counter-propagating laser beams (diameter $\approx 500\ \mu$m) at a wavelength of 1064 nm with a total power of 2 W. We use the lattice as an elevator to transport the ultracold atoms upwards into the center of the Paul trap, which is located 30 cm above the quadrupole Ioffe configuration trap. The lattice is moved by changing the relative detuning of the two beams in a controlled manner [17]. The transport efficiency reaches more than 60%. During transport the depth of the lattice is sufficiently small ($\approx k_B \times 10\ \mu$K) so that evaporation keeps the atom temperature at about $1\ \mu$K. After transport the atomic sample is loaded into a crossed optical dipole trap ($\lambda = 1064$ nm). By lowering the trap depth, we evaporatively cool the atoms and end up with a Bose-Einstein condensate (BEC) of about 10^5 atoms confined in a dipole trap with trap frequencies of about $\omega_{\mathrm{Rb}}^{(x,y,z)} = (60, 60, 8\ \mathrm{Hz})$. The condensate is detected via standard absorption imaging.

The BEC is initially located about 300 μm away from the ion. We move the ion within 2 ms along the Paul trap axis (x axis) into the BEC by changing the end cap voltages. The cooling lasers for the ion are switched off in order to ensure that the ion relaxes into its electronic ground state $|F = 1/2, m_F = \pm 1/2\rangle$ and to avoid changes in the atom-ion collision dynamics due to the cooling radiation.

Initially, the temperature of the ion is on the order of a few mK, which is much larger than the optical trap depth of about $k_B \times 1\ \mu$K. Thus almost any collision with a cold atom leads to the atom being lost from the trap. As a consequence, one could naively expect that the atom loss stops after a few collisions, once the ion is sympathetically cooled to atomic temperatures. However, when we measure the number of Rb atoms remaining in the trap as a function of the interaction time, we find a continuous loss of atoms (Fig. 2). It is the driven micromotion [18] of the rf trap which is responsible for this continuing loss. In an atom-ion collision, energy can be redistributed among all motional degrees of freedom, enabling also the flux of micromotion energy to secular motion. After each collision, micromotion is quickly restored by the driving rf field. An equilibrium between the energy that is inserted by the driving field and the energy taken away by the lost atoms is reached within a few collisions. Thus the minimal temperature of a sympathetically cooled ion stored in a rf trap is determined by the amount of micromotion of the ion [19]. Stray electric fields which shift the ion position away from the zero of the rf potential increase micromotion, leading to the so-called excess micromotion [18]. By applying dc electric fields along the radial direction, this part of the micromotion is tunable.

Figure 2 shows the elastic collision measurements with either (a) a thermal cloud of atoms (temperature $T_{\mathrm{Rb}} = 80$ nK, which is just above T_c) or (b) a BEC. In the following, we analyze these data in detail starting out with the case for thermal atoms. In general, the atom losses in our experiment are predominantly determined by atom-ion collisions. The lifetime of the atom sample without an ion being present exceeds 15 s. The loss of atoms is then described by $\dot{N} = -\tilde{n}\sigma_{\mathrm{el}} v_I$, where $\tilde{n}$ is the density of the atom cloud at the position of the ion, σ_{el} the elastic atom-ion cross section, and v_I the velocity of the ion. In principle, all three quantities are unknown. Based on our measurements and additional constraints of the following model, we can still give estimates for them.

It is important to note that the density profile of the atom cloud is depleted locally due to the collisions with the well-localized ion. According to its mass m_I, energy $E_I = m_I v_I^2/2$, and trap frequency ω_I, the ion will be localized inside a region (which for simplicity we choose to be spherical) of radius $r_0 = \sqrt{E_I/m_I\omega_I^2}$. Inside this sphere, we assume a homogeneous density $\tilde{n}$. Right outside the sphere, the density is given by $n = N\bar{\omega}_{\mathrm{Rb}}^3(m_{\mathrm{Rb}}/2\pi k_B T_{\mathrm{Rb}})^{3/2}$, which is the peak density of a thermal cloud of Rb atoms (mass m_{Rb}) confined in a harmonic trap with mean trap frequency $\bar{\omega}_{\mathrm{Rb}} = (\omega_{\mathrm{Rb}}^{(x)}\omega_{\mathrm{Rb}}^{(y)}\omega_{\mathrm{Rb}}^{(z)})^{1/3}$. The measured atom loss $\dot{N}$, which at $t = 0$ is $\dot{N} = 1.5 \times 10^4\ \mathrm{s}^{-1}$ (as can be read off from Fig. 2), must match the net flux of atoms into the "sphere of depletion," leading to the balance condition $\dot{N} = \pi r_0^2(n - \tilde{n})v_{\mathrm{th}}$. Here the thermal velocity of the atoms is given by $v_{\mathrm{th}} = \sqrt{k_B T_{\mathrm{Rb}}/8\pi m_{\mathrm{Rb}}}$. By setting $\tilde{n} = 0$ in the balance condition we get a lower bound for the ion energy, which for our parameters is equal to $k_B \times 17$ mK. We can also estimate an upper limit of the ion energy from our method of compensating micromotion. The compensation is based on minimizing the position shift of the ion when the rf amplitude is changed. With this method we can reduce the dc electric field at the position of the ion to below 4 V/m, corresponding to a maximum ion energy of $k_B \times 40$ mK [18]. By taking the midpoint between the two bounds we estimate the ion energy to be about $k_B \times 30$ mK. Plugging this energy into the expressions above we get $r_0 \approx 1.45\ \mu$m and a density of $\tilde{n} \approx 0.45n$. Moreover, we can determine the cross section σ_{el} to be $1.9 \times 10^{-14}\ \mathrm{m}^2$. This value is in rough agreement with the semiclassical estimate $\sigma_{\mathrm{el}}^{\mathrm{semi}} = 9 \times 10^{-15}\ \mathrm{m}^2$.

A slightly different analysis has to be done for the measurement with the BEC shown in Fig. 2(b). Again, collisions of the atoms with the trapped ion will lead to a sphere of depletion within the condensate. However, the flux of atoms into the sphere is now driven by mean field pressure rather than thermal motion. From numerical calculations using a 3D Gross-Pitaevskii equation with an absorptive (imaginary) potential term, we find that the flux into the sphere can be approximated by $4\pi r_0^2 \tilde{n} v_e$, as long as $\tilde{n} \gtrsim 0.1n$. Here $v_e = 4\hbar\sqrt{2\pi a(n - \tilde{n})}/m_{\mathrm{Rb}}$ is the velocity with which the atoms enter the sphere, $a = 5.61$ nm is the Rb-Rb s-wave scattering length, and $n = (15m_{\mathrm{Rb}}^3\bar{\omega}_{\mathrm{Rb}}^3 N/\hbar a^{3/2})^{2/5}/8\pi$ is the peak density of the condensate. By equating the net flux to the measured loss rate of the BEC at $t = 0$, $\dot{N} = 8 \times 10^4\ \mathrm{s}^{-1}$ (see Fig. 2), we find that the ion energy has to be larger than $k_B \times 1$ mK. Our analysis shows that, on the other hand, the ion energy has to be smaller than in the thermal case. Indeed, to minimize the temperature of the trapped ion, a comparatively large effort was made to compensate micromotion for the experiments with the BEC. Given that $\sigma_{\mathrm{el}}/\sigma_{\mathrm{el}}^{\mathrm{semi}} \approx 2$ as in the thermal case, our data suggest a reasonable ion energy of about $k_B \times 5$ mK. This implies $r_0 \approx 0.8\ \mu$m, a density of $\tilde{n} \approx 0.1n$, and a cross section of $\sigma_{\mathrm{el}} \approx 3.1 \times 10^{-14}\ \mathrm{m}^2$. We also measured the loss rate for a single Rb^+ ion and found it to be about the same as with Ba^+ (Fig. 2). This is not surprising, since the atom loss rate depends only weakly on the ionic mass and the inner structure of the ion is irrelevant in the semiclassical regime.

When we intentionally increase the dc electric field $\mathcal{E}_{\mathrm{dc}}$, we expect the atom loss rate to rise for two reasons. First, the atom-ion scattering rate rises as $|\mathcal{E}_{\mathrm{dc}}|^{1/3}$ (see also [12]); second, as the sphere of depletion increases, its depletion is reduced. Figure 3 shows an increase of the loss rate up to an electric field of $\mathcal{E}_{\mathrm{dc}} \approx 30$ V/m, where the amplitude of the ion's secular motion is $r_0 \approx 20\ \mu$m. This value is comparable to the size of the atom cloud, which has an extension of about 15 μm along the radial and 80 μm along the axial direction. The model of a well-localized ion and a sphere of depletion is clearly no longer valid in this regime. We explain the decrease of the atom loss rate for even higher fields by the fact that the ion spends a significant amount of time in regions of lower atom density.

In addition to the elastic processes discussed so far, we have also investigated inelastic atom-ion collisions. For this we load two $^{138}Ba^+$ ions into the ion trap. Typically after a time corresponding to 10^4–10^5 elastic atom-ion collisions, the fluorescence of one of the Ba^+ ions is lost (Fig. 4). Since the position of the remaining bright Ba^+ ion does not change, we infer that the other Ba^+ ion has been replaced by an unknown dark ion formed in a reaction. We can determine the mass m_I of the dark ion by measuring the radial trap frequency. For this we modulate the amplitude of the rf voltage. When the modulation frequency is close to the trap frequency, the ion motion is resonantly excited and a drop of the Ba^+ fluorescence signal is observed. We observe only two resonance frequencies at 245 and 400 kHz. Ba^+ gives rise to the resonance at 245 kHz (which simply equals the Ba^+ trap frequency that was chosen for these particular measurements). Since the radial trap frequency scales as $1/m_I$ [20] (and since there is comparatively weak coupling between the ions due to $\omega_{I,\mathrm{ax}} \ll \omega_{I,\mathrm{rad}}$), the 400 kHz resonance

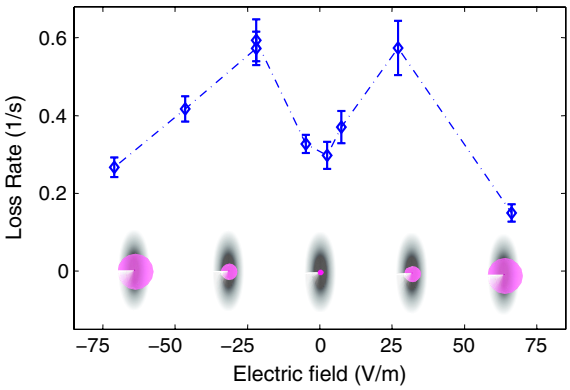

FIG. 3 (color online). Loss rate of a thermal atom cloud when a static electric field is applied. The loss rate is minimal for zero electric field and has a maximum at about 30 V/m.

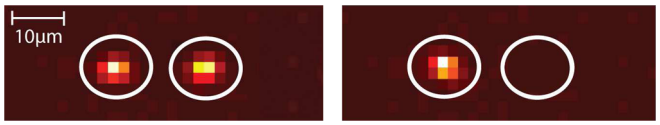

FIG. 4 (color online). Left: Fluorescence image of two Ba^+ ions. Right: Fluorescence of one $^{138}Ba^+$ next to an unknown dark ion . We infer the existence of the dark ion from the position of the Ba^+.

corresponds to the mass of $^{87}Rb^+$. We conclude that the dominant inelastic process in our system is the charge transfer process $Rb + Ba^+ \rightarrow Rb^+ + Ba$ with a cross section $\sigma_{\text{ch.ex.}}$ ranging between 10^{-19} and 10^{-18} m^2. So far we have not observed the formation of molecular ions. Our charge transfer results are comparable to the ones observed for the heteronuclear case of (Rb, Yb^+) [13]. Homonuclear charge transfer rates are orders of magnitudes higher [11]. In our case the charge transfer is predicted to be dominantly radiative, where a photon carries away most of the 1 eV of energy released in this reaction [21].

We now show how a single ion may be used to locally probe the atomic density distribution. By controlling the end cap voltage we vary the position of the single Rb^+ ion relative to the atom sample. At each position x the atom loss is measured on a freshly prepared atom cloud for a given interaction time (Fig. 5). The measurement is performed for three different condensate fractions. We can theoretically reproduce the data shown in Fig. 5 with our model, which demonstrates our quantitative understanding of the dynamics. For this we write the total atom loss of a partly condensed cloud as a sum of the individual losses from the BEC and the thermal cloud as discussed before. For numerical calculations we choose $\sigma_{\text{el}} = 3 \times 10^{-14}$ m^2

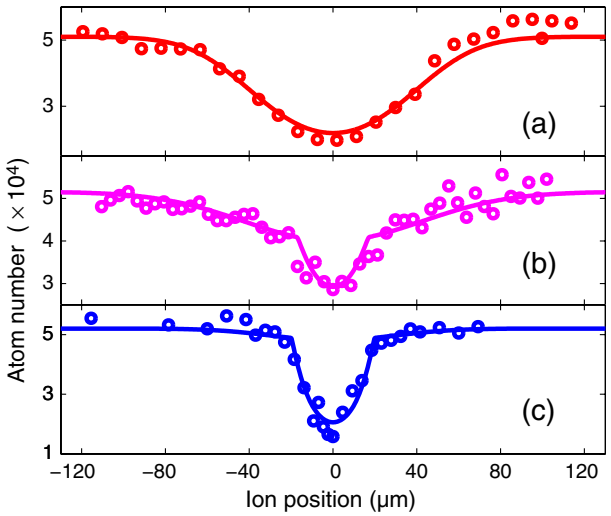

FIG. 5 (color online). Number of Rb atoms remaining in the trap depending on the position of the Rb^+ ion relative to the center of the atom cloud. The measurement is performed with (a) a thermal cloud, (b) a partially condensed cloud, and (c) an almost pure Bose-Einstein condensate. The interaction time was (a) 1.5, (b) 1, and (c) 0.5 s. The solid lines are fits, where the ion energy E_I and the atom temperature T_{Rb} are used as free fit parameters.

and make use of the well-known density profiles for a thermal and a condensed atom cloud confined in a harmonic trap. The thermal component and BEC are in equilibrium and obey $N_c/N = 1 - (T_{\text{Rb}}/T_c)^3$, where T_c is the critical temperature and N_c/N is the condensate fraction which changes with time. The temperature T_{Rb} of the atomic sample is constant, as determined by the optical trap depth. It is used as a free fit parameter in our model together with the ion energy E_I, which we keep fixed for all three measurements. Figure 5 depicts the total number of remaining particles $N(x)$ as a function of the ion's position x. The values for T_{Rb} obtained from the fit (a) 50, (b) 35, and (c) 25 nK are in nice agreement with the temperatures determined separately in time-of-flight measurements. Moreover, the fit suggests $E_I \approx k_B \times 14$ mK, which is in the same range as the temperatures found in the Ba^+ experiments. The ion probe features a spatial resolution on the micrometer scale and has advantages compared to absorption imaging which integrates over the line of sight.

The authors thank Albert Frisch and Sascha Hoinka for their help during the early stage of the experiment and Thomas Busch, Tommaso Calarco, Robin Côté, Bretislav Friedrich, Bo Gao, Zbigniew Idziaszek, Tobias Schätz, Wolfgang Schnitzler, and Jaques Tempère for helpful discussions and support. We are grateful to Rudi Grimm for generous support and to Michael Drewsen and the group of Rainer Blatt for advice on the design of the ion trap. This work was supported by the Austrian Science Fund (FWF). S. S. acknowledges support from the Austrian Academy of Sciences.

[1] R. Côté, Phys. Rev. Lett. **85**, 5316 (2000).
[2] P. Massignan, C. J. Pethick, and H. Smith, Phys. Rev. A **71**, 023606 (2005).
[3] R. M. Kalas and D. Blume, Phys. Rev. A **73**, 043608 (2006).
[4] F. M. Cucchietti and E. Timmermans, Phys. Rev. Lett. **96**, 210401 (2006).
[5] R. Côté, V. Kharchenko, and M. D. Lukin, Phys. Rev. Lett. **89**, 093001 (2002).
[6] P. F. Staanum *et al.*, Nature Phys. **6**, 271 (2010).
[7] T. Schneider *et al.*, Nature Phys. **6**, 275 (2010).
[8] C. Chin *et al.*, Rev. Mod. Phys. **82**, 1225 (2010).
[9] Z. Idziaszek *et al.*, Phys. Rev. A **79**, 010702 (2009).
[10] M. Cetina *et al.*, Phys. Rev. A **76**, 041401 (2007).
[11] A. T. Grier *et al.*, Phys. Rev. Lett. **102**, 223201 (2009).
[12] C. Zipkes *et al.*, Nature (London) **464**, 388 (2010).
[13] C. Zipkes *et al.*, preceding Letter, Phys. Rev. Lett. **105**, 133201 (2010).
[14] R. Teachout and R. Pack, Atomic Data **3**, 195 (1971).
[15] R. Côté and A Dalgarno, Phys. Rev. A **62**, 012709 (2000).
[16] G. Thalhammer *et al.*, Phys. Rev. A **71**, 033403 (2005).
[17] S. Schmid *et al.*, New J. Phys. **8**, 159 (2006).
[18] D. J. Berkeland *et al.*, J. Appl. Phys. **83**, 5025 (1998).
[19] F. G. Major and H. G. Dehmelt, Phys. Rev. **170**, 91 (1968).
[20] D. Wineland *et al.*, J. Res. Natl. Inst. Stand. Technol. **103**, 259 (1998).
[21] O. P. Makarov *et al.*, Phys. Rev. A **67**, 042705 (2003).